Cardiol Young 2003; 13: 352–360

ISSN 1047-9511

Original Article

Predictors of residual defects following closure of defects in the oval fossa using the Amplatzer device: echocardiography recapitulates morphometry

Duraisamy Balaguru,[1] Robert H. Anderson,[2] Geoffrey L. Rosenthal,[3] Andrew C. Cook,[2] Wolfgang A.K. Radtke,[1] Girish S. Shirali[1]

[1]*Department of Pediatrics (Cardiology), Medical University of South Carolina, Charleston, South Carolina, USA;* [2]*Institute of Child Health, University College, London, United Kingdom;* [3]*Cleveland Clinic Foundation, Cleveland, Ohio, USA*

Abstract *Objectives:* This study was designed to identify predictors of residual defects following deployment of the Amplatzer device to close septal defects within the oval fossa. *Methods:* Between February 1997 and February 2000, we used the Amplatzer device to close defects in the oval fossa in 89 patients. Of these patients, 18 (20%) had residual defects. At 6 or 12 months following placement of the device, 13 defects (14.6%) had persisted. We evaluated several variables derived from clinical features, transesophageal echocardiography and catheterization to establish predictors for residual shunting. *Results:* Multivariate analysis identified a shorter superior rim of less than 8 mm (Odds ratio = 10.1; 95% confidence intervals = 2.64–38.72; p = 0.001), and a smaller interatrial septum in the 30-degree transesophageal echocardiographic plane of less than 30 mm (Odds ratio = 5.5; 95% confidence intervals = 1.17–26.14; p = 0.03) as independent predictors of residual defects. When the analysis was repeated defining only those 13 patients with persisting residual defects at 6 or 12 months as failures, a short superior rim (p = 0.004) remained a predictor for residual shunting. *Conclusions:* Defects with a short superior rim and smaller interatrial septum in the 30-degree transesophageal echocardiographic plane independently and additively predict an increased probability of residual shunting following closure of defects in the oval fossa using the Amplatzer device.

Keywords: Atrial septal defect; interventional catheterization; echocardiography

The past 20 years have seen an increasing body of experience with transcatheter closure of atrial septal defects. The United States Food and Drug Administration has recently approved the Amplatzer occluder for closure of such defects. The device is safe and effective, but some concerns remain.[1–3] Residual flow across the defect, albeit minimal, has previously been reported in between one-tenth and three-fifths of patients following this procedure.[1,4] Even a small residual defect may constitute a potential substrate for future paradoxical embolism. Complete closure of the defect, therefore, remains the objective of any technique, whether transcatheter or surgical. Identification of independent factors that predict the occurrence of residual shunting, and understanding the morphologic basis for the residual defects, would be an important step towards improving optimal selection of patients for closure.

To the best of our knowledge, there are no published studies examining predictors of success or failure of complete closure using the Amplatzer device. The current study was designed to identify independent predictors of residual shunting in these patients, using variables derived from clinical features, transesophageal echocardiography and catheterization.

Correspondence to: Girish Shirali MBBS, FACC, FAAP, The Children's Heart Program, 165 Ashley Avenue, P.O. Box 250915, Charleston SC 29425, USA. Tel: +843 792 3279; Fax: +843 792 5878; E-mail: shiralig@musc.edu

Accepted for publication 16 January 2003

The morphologic basis of the echocardiographic findings was then explored in the setting of gross anatomy.

Methods

Patients studied

The population included all patients who underwent closure of interatrial communications within the oval fossa, or patent oval foramens, using the Amplatzer atrial septal defect occluder in our institution between February 1997 and February 2000. All eligible patients underwent transesophageal echocardiography and cardiac catheterization under general anesthesia with endotracheal intubation.

Echocardiographic evaluation

All patients underwent multiplane transesophageal echocardiography using one of three probes [Vingmed pediatric (6.0 MHz) – Vingmed Sound, Horton, Norway, ATL Apogee (5.0 MHz) – ATL Incorporated, Bothell, Washington or Hewlett-Packard Omniplane II (5.0/6.2 MHz) – Hewlett-Packard, Andover, Massachusetts]. The technique for insertion of the probes, and the protocol for assessing cardiac morphology and function, followed previously described guidelines.[5–7] Images were obtained in multiple planes to visualize optimally the surrounds of the oval fossa, and defects within it. Each study was recorded in its entirety onto super-video home system videotape and analyzed on-line and off-line.

Maximum diameters of the defect were recorded in at least two orthogonal planes. The rims of the fossa were measured from the closest edge of the defect to the following landmarks:

- The superior cavoatrial junction (superior rim).
- The inferior cavoatrial junction (inferior rim).
- The septal hinge points of the leaflets of the tricuspid and mitral valves.
- The junction of the right upper pulmonary vein with the left atrium.
- The junction of base of the primary atrial septum and the left atrial floor postero-inferiorly (posterior-inferior rim).
- The aortic root (aortic rim).

For patients with multiple defects, each defect was evaluated individually. The length of the entire floor of the oval fossa, representing the primary atrial septum, was measured in 3 transesophageal echocardiographic planes: 0, 30 and 90 degrees. The 0-degree plane corresponds to a slightly foreshortened transthoracic apical view. This measurement was made between the septal hinge of the tricuspid valve and the junction of the roof of the atriums with the atrial septum. The length of the septum at 30 degrees was measured at the level of the aortic sinuses (Fig. 1). This corresponds to the portion that interposes between the aortic root and the superior cavo-atrial junction. The length of the septum at 90 degrees corresponds to the portion between the orifices of the superior and inferior caval veins at their junctions with the right atrium. In our institution, patients were excluded from consideration for closure using the Amplatzer device if any rim other than the aortic rim measured less than 5 mm in length. Closure was performed, however, in absence of any measurable aortic rim.

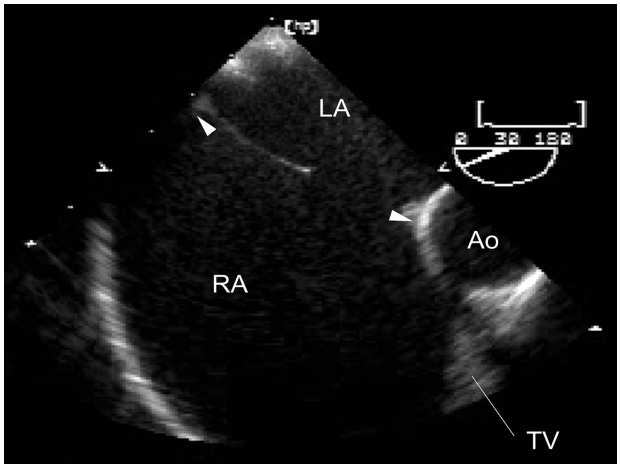

Figure 1.
Multiplane transesophageal echocardiographic view: 30-degree plane of section at the level of the aortic root showing the width of the oval fossa behind the aorta (between arrowheads). Ao: aorta; LA: left atrium; RA: right atrium; TV: tricuspid valve.

Cardiac catheterization

Cardiac catheterization included baseline hemodynamic assessment and angiographic delineation of anatomy, as previously described elsewhere.[8] Using fluoroscopic and echocardiographic visualization, a sizing balloon catheter was used to measure the pull-through stretched diameter of the defect. The final decision regarding number and size of device(s) to be used was based on data obtained from echocardiography and catheterization. Thus, the echocardiographic characteristics of the defect, and the nature of the rims surrounding it, were evaluated in the context of the measured stretched diameter of the defect and the width of the oval fossa.

The Amplatzer atrial septal defect occluder (AGA Medical Corporation, Golden Valley, Minnesota) was used in all patients. This device has been extensively described in prior studies.[1,8,9] Fluoroscopy and echocardiography provided real-time guidance of deployment.[1]

https://doi.org/10.1017/S1047951103000714 Published online by Cambridge University Press

Collection of data

All scans obtained during placement and follow-up echocardiographic data were reviewed by two of the investigators (D. Balaguru, G. Shirali). Demographic and clinical data included age, gender, weight, height, body surface area, prior cardiac surgery, and presence of a true defect as opposed to a patent foramen. Echocardiographic measurements included number of defects, their diameter in 2 orthogonal planes, length of each rim around each defect, width of tissue bridge separating multiple defects, and the width of the oval fossa as measured in the planes taken at 0, 30 and 90 degrees. The ratio of pulmonary to systemic flows, the stretched diameter of the defect, and the diameter of the device were obtained from catheterization records.

Echocardiographic calculations

The cross-sectional area of the defect was calculated using the formula, area $= \pi r^2$, when the orthogonal diameters were equal, or area $= \pi(d_1/2) \times (d_2/2)$ when the orthogonal diameters were unequal, with r representing radius and d diameter. The cross-sectional area and the largest diameter of the defect, the width of the floor of the fossa in each of the three planes, and the diameter of the device were indexed to body size. Measurements of area were indexed to body surface area, and linear measurements were indexed to the square root of body surface area.[10] Shape, stretchability, and size of the defect relative to the size of the device were evaluated using calculated indexes. The circularity index was defined as the ratio of major and minor diameters measured by echocardiography. The stretchability index was defined as the ratio of the balloon stretched diameter to the major diameter of the defect measured by echocardiography. The sizing index was expressed as the ratio of the diameter of the device to the stretched diameter of the defect measured by echocardiography.

Follow-up

Transthoracic echocardiography was used for follow-up studies. All patients underwent echocardiography on the day after deployment of the device. Subsequent clinical, radiological and echocardiographic follow-up was obtained 6 months later, and then annually. Echocardiograms demonstrating residual defects were reviewed to evaluate the size and location of the defect.

Definition of study groups

Patients with a residual defect of any size detected by echocardiography at any time during the first year after placement of the device were classified as failures. Patients who had no residual defect detected at any time during the first year after placement of the device were classified as successes. A second set of analyses was also performed, redefining the failures as those patients who had a residual defect at either 6 or 12 months after placement of the device.

Statistical analysis

Contingency table analyses were performed to assess associations between dichotomous independent variables and the occurrence of residual defects. Chi-square and Fisher's exact tests were used to determine statistical significance. The associations between continuous variables and residual defects were evaluated using simple logistic regression. In this exploratory study, an alpha level of 0.10 was used to reject the null hypothesis for the univariate analysis. Stepwise multivariable logistic regression was performed to evaluate the independent effects of variables that were found to be associated with residual defects based upon univariate analysis. An alpha level of 0.05 was used to reject the null hypothesis for the multivariate analysis. For both continuously scaled independent variables, a sensitivity analysis was performed to determine the threshold for increased risk of failure. No adjustments were made for multiple comparisons. All analyses were performed using SAS version 6.12 (SAS Institute Inc., SAS/STAT, Version 6.12, Cary, North Carolina, 2000).

Results

During the period of study period, we evaluated 104 patients by transesophageal echocardiography for possible closure of atrial septal defects or patent oval foramens with a device. Of these, 15 patients were ineligible. The reasons were inadequate inferior rims in 8 patients, multiple fenestrations in 2 patients, and because the calculated size of device either exceeded the width of the oval fossa in 3 patients, or was not commercially available at the time in the remaining 2 patients.

Closure was attempted, therefore, in 89 patients during the period of study. Demographic and clinical data for all patients are summarized in Table 1. Overall, 18 of the 89 (20.2%) patients had residual defects at some time during follow up. In 13 patients, a residual defect was noted either at 6-months or 1-year after insertion of the device. The locations of residual defects were widely variable. The residual defect was 3 mm or less in diameter in all but one patient. In this patient, the residual defect was eventually closed with a second device.

Univariate analysis

Variables associated with occurrence of residual defects were initially identified by univariate analysis

https://doi.org/10.1017/S1047951103000714 Published online by Cambridge University Press

for categorical (Table 2) and continuous (Table 3) variables respectively. We found the following variables to be significant predictors of residual defects:

- Shorter length of the interatrial septum as measured in the 30-degree transesophageal echocardiographic plane ($p = 0.04$).
- A smaller rim to the tricuspid valve ($p = 0.04$) and mitral valve ($p = 0.06$).
- The need for multiple devices ($p = 0.06$).
- A smaller superior rim ($p = 0.07$).
- A higher ratio of pulmonary to systemic flow ($p = 0.07$).

Among the variables indexed to body surface area, a larger device ($p = 0.05$), a larger major diameter of the defect ($p = 0.08$), and a longer length of the interatrial septum at the 0-degree transesophageal echocardiographic plane ($p = 0.09$), all predicted residual defects.

Multivariate analysis

Predictors identified by univariate analysis constituted the candidate variables for the multivariate analysis by stepwise multiple logistic regression. This analysis identified a smaller length of the superior rim (odds ratio = 10.1, 95% confidence intervals = 2.64–38.72; $p = 0.001$), and a smaller length of the interatrial septum as measured in the 30-degree transesophageal echocardiographic plane (odds ratio = 5.5, 95% confidence intervals = 1.17–26.14; $p = 0.03$) as independent predictors of residual defects. For both variables, the predictive model held true only for absolute, and not for indexed, measurements.

Table 1. Demographics and clinical data for all 89 patients.

Variable	Median (range)
Age (years)	9.5 (1.4–88)
Weight (kg)	37.8 (8.7–137)
Height (cm)	134 (79–186)
Body surface area (m^2)	1.1 (0.45–2.4)
Gender (male : female)	35 : 54
Diagnosis (patent oval foramen : atrial septal defect)	8 : 81
Ratio of pulmonary to systemic flow	1.7 (0.8–6.0)
Association with atrial septal aneurysm (n)	14 (15.7%)
Multiple defects (n)	17 (19.1%)
Previous heart surgery for structural heart defect (n)	6 (6.7%)
Follow-up (months)	12.1 (0.03–38.5)

Threshold values for independent predictors

In order to evaluate the independent predictors of residual defects in a clinically usable format, we computed a threshold value for each of the independent variables by performing a sensitivity analysis. The threshold for the superior rim was 8 mm. Of 13 patients with this rim shorter than 8 mm, 8 (61.5%) had a residual defect, compared to 10 of 75 patients (13.3%) in whom this rim was equal to or longer than 8 mm (odds ratio 10.11, 95% confidence intervals 2.64–38.72, $p = 0.001$). The length of the superior rim was unavailable for one patient undergoing successful closure.

The threshold for the width of the oval fossa as measured in the 30-degree plane was 30 mm. Of 51 patients with this part of the fossa measuring less than 30 mm, 13 (25.4%) had a residual defect, compared to 2 of 30 patients (6.6%) in whom the width of the fossa exceeded 30 mm (odds ratio 5.5, 95% confidence intervals 1.17–26.14, $p = 0.03$). The width of the fossa in the 30-degree plane could not be measured in 6 patients, 5 undergoing successful closure and 1 having a residual defect.

Regression equation and statistical model

The relationship between the two independent variables judged as dichotomous variables using their respective threshold values, and the probability of residual shunting, was described by the following equation:

$$p = \frac{1}{1 + e^{\left[\begin{array}{c}-(-3.1764 + (\text{superior rim value} \times 2.3578)) \\ + (30\text{-degree value} \times 1.5528))\end{array}\right]}}$$

where 'superior rim value' is 1 for a superior rim equal to or longer than 8 mm, and is 0 for a superior

Table 2. Predictors of residual defects. Univariate analysis, categorical variables.

Parameter	Success (n = 71)	Failure (n = 18)	Odds ratio for failure	95% confidence intervals	p value
Gender (female : male)	43 : 28	11 : 7	1.02	0.81–1.24	0.97
Patent foramen ovale : atrial septal defect	7 : 64	1 : 17	0.64	0.07–5.66	0.68
Atrial septal aneurysm (n)	10 (14.1%)	4 (22.2%)	1.74	0.48–6.38	0.40
Multiple defects (n)	12 (16.9%)	5 (27.8%)	1.89	0.57–6.30	0.29
Multiple devices (n)	3 (4.2%)	3 (16.7%)	4.53	0.83–24.00	0.06
Previous heart surgery (n)	1 (1.4%)	3 (16.7%)	3.35	0.68–16.56	0.12

https://doi.org/10.1017/S1047951103000714 Published online by Cambridge University Press

Table 3. Predictors of residual defects. Univariate analysis, continuous variables.

Parameter	Success (n = 71) Median (range)	Failure (n = 18) Median (range)	p value
Age (years)	8.5 (1.4–72.5)	10.4 (1.9–88.1)	0.38
Weight (kg)	38.4 (10.3–137)	22.3 (8.7–93.4)	0.15
Height (cm)	137 (79–186)	114 (79.5–175)	0.13
Body surface area (m^2)	1.22 (0.48–2.40)	0.9 (0.5–2.2)	0.17
Ratio of pulmonary to systemic flows	1.7 (0.8–4.30)	1.9 (1.3–6.0)	0.07
Superior rim (mm)	12 (5–27)	9.5 (4–36)	0.07
Inferior rim (mm)	18 (6.5–38)	16.5 (6–35)	0.97
Tricuspid valve rim (mm)	14.5 (7–38)	12 (7–23)	0.04
Mitral valve rim (mm)	13 (6–35)	10 (7–15)	0.06
Right upper pulmonary vein rim (mm)	13 (6–35)	12 (7–19)	0.21
Aortic rim (mm)	4.9 (0–23)	3 (0–14)	0.18
Postero-inferior rim (mm)	13 (5–33)	15 (8–30)	0.36
Length of atrial septum in 0-degree plane (mm)	33 (21–53)	32 (17–47)	0.42
Length of atrial septum in 0-degree plane indexed to square root of body surface area (mm/m)	30.5 (13–78)	35.4 (23–86)	0.25
Length of atrial septum in 90-degree plane (mm)	32 (22–57)	29.5 (20–47)	0.21
Length of atrial septum in 90-degree plane indexed to square root of body surface area (mm/m)	30.6 (21–70)	32.7 (20.4–41.9)	0.95
Length of atrial septum in 30-degree plane (mm)	27 (17–45)	26 (17–32)	0.04
Length of atrial septum in 30-degree plane indexed to square root of body surface area (mm/m)	25.7 (18–55)	25.5 (17–35.7)	0.60
Major diameter of defect (mm)	10 (1–27)	10 (4–24)	0.50
Major diameter of defect indexed to square root of body surface area (mm/m)	10.7 (0.9–24)	12.9 (5.4–26.4)	0.16
Minor diameter of defect (mm)	8.5 (1–20)	9 (3–19)	0.81
Minor diameter of defect indexed to square root of body surface area (mm/m)	8.65 (0.8–17.4)	9.8 (3.8–18.9)	0.35
Cross-sectional area of defect (mm^2)	70.7 (7–361)	70.7 (11.8–340)	0.90
Cross-sectional area of defect indexed to body surface area (mm^2/m^2)	75.6 (5.4–249)	87 (18.7–373)	0.32
Stretched diameter (mm)	16 (4–32)	15.5 (6–28)	0.53
Stretched diameter of defect indexed to square root of body surface area (mm/m)	15.7 (3.0–24.7)	14.6 (7.3–31.4)	0.09
Diameter of device (mm)	16 (5–32)	16 (6–26)	0.73
Diameter of device indexed to square root of body surface area (mm/mm)	16.9 (6–26)	17.1 (9.9–30.7)	0.13
Diameter of device/major diameter of defect	1.5 (1.0–5.7)	1.5 (1.1–2.4)	0.27
Diameter of device/longest length of interatrial septum	0.5 (0.2–0.8)	0.5 (0.2–0.8)	0.20
Circularity index (major diameter/minor diameter of defect)	1.25 (1.0-2.43)	1.2 (1.0–2.0)	0.40
Stretchability index (stretched diameter/unstretched major diameter of defect)	1.5 (0.9–5.3)	1.5 (1.1–2.4)	0.31
Device sizing index (diameter of device/stretched diameter of defect)	1.0 (0.9–2.0)	1.0 (0.8–1.2)	0.27

Table 4. Prediction of probability of residual shunting by statistical model. Independent predictors of failure are used as dichotomous variables using their threshold values.

Predictors	Prediction by statistical model [probability of residual defect]	Internal validation [observed residual defect/ total in group (%)]
Superior rim equal to or longer than 8 mm, and width of oval fossa at 30 degrees equal to or longer than 30 mm	0.04	1/27 (3.7%)
Superior rim equal to or longer than 8 mm, and width of oval fossa at 30 degrees less than 30 mm	0.16	7/42 (16.7%)
Superior rim less than 8 mm, and width of oval fossa at 30 degrees equal to or longer than 30 mm	0.31	1/3 (33.3%)
Superior rim less than 8 mm, and width of oval fossa at 30 degrees less than 30 mm	0.68	6/9 (67.7%)

https://doi.org/10.1017/S1047951103000714 Published online by Cambridge University Press

rim shorter than 8 mm; and where "30-degree value" is 1 for an interatrial septal length at 30 degrees equal to or longer than 30 mm, and is 0 for a length less than 30 mm.

Using this regression formula for the two dichotomous independent predictors, we were able to provide a predictive model. For internal validation of the model, all patients from our study were categorized into one of these four groups based on these measurements. The predictive models, and the results of internal validation, are summarized in Table 4.

Re-analysis excluding patients with residual defects seen only on the first day

Many investigators consider residual defects only those seen on the first day following attempted closure, deeming those not seen subsequently as insignificant. We repeated the analysis, therefore, reclassifying such patients as having undergone successful closure. The 13 remaining patients had a residual defect at either 6 or 12 months after placement of the device. Subsequent to this analysis, only a short superior rim of less than 8 mm remained a significant predictive factor of residual defects ($p = 0.004$).

Discussion

We have used two sets of criterions to define failure of complete closure of defects within the oval fossa. The first set, based on recognition of a residual defect of any size as failure, is based on the premise that any defect may be a substrate for future paradoxical embolism, even though the shunt may be hemodynamically insignificant. The second set is based on less stringent criterions for failure of complete closure. In this second set, we counted as successes all those patients who had a residual defect only on the first day subsequent to attempted closure. We discovered that a short superior rim emerged as a statistically significant predictor with both sets of analyses. A short width of the oval fossa as measured in the 30-degree plane was a significant predictor only when analyzing all patients with any degree of residual shunting. We sought to obtain morphologic correlation to these statistically significant variables.

Morphologic correlation of the statistical predictors

Martins and Anderson[11] have recently reviewed the morphology of the interatrial septum in the context of interventional closure. They describe the interatrial septum and its surrounds as consisting of either "walls" or "folds". "Walls" comprise the true septal structures interposed between the cavities of the two atriums. If a wall were pierced or excised from within an atrium, the result would be to create a communication with the other atrium. Such walls are represented by the flap valve of the oval fossa, and by the antero-inferior muscular rim on which the flap valve is hinged. In contrast, "folds" consist of parietal walls of the heart that have folded on themselves to produce the larger part of the surrounds of the oval foramen. If a fold were pierced or excised, the result would be a communication with the extracardiac space. Apart from the antero-inferior part on which the flap valve is hinged, most of the remaining rims of the oval fossa, structures currently considered by many to represent the "septum secundum", consist of folds rather than true walls.

The superior rim

The superior rim of a defect within the oval fossa is exclusively a fold extending alongside the mouth of the superior caval vein, between the attachments of the caval vein to the right atrium and the right upper pulmonary vein to the left atrium. In normal hearts, this is usually the most obvious and best-formed area of the circumference of the oval fossa (Fig. 2). If this rim were short in a patient with a septal defect (Fig. 3), it is conceivable that the device may not have adequate support. The resultant interference with the self-centering mechanism, or with the ability of the two discs to appose completely, might lead to a residual defect. While the current statistical derivation demonstrates the association of a short rim in this location with a higher incidence of residual defects, this proposed mechanism remains speculative. The fact that the absolute length of the superior rim, and not the length of the rim indexed to body surface area, was a predictive factor probably indicates that the mechanism of residual defect is related to the size and shape of the device, and the anatomy of the surrounds of the oval fossa itself, rather than to the size of the patient.

Width of the oval fossa in the 30 degree transesophageal echocardiographic plane. When the superior rim is traced anteriorly, the circumference of the oval fossa continues as the anterior rim that is adjacent to the aortic root. If this infolding were shallow, it may not provide much support to the device. It is this rim that forms a significant part of the margins of the oval fossa that are seen in the 30-degree plane (Figs 4 and 5).

We found that a short superior rim was additive to the effect of a short width of the oval fossa as seen in the 30-degree plane in their association with failure of complete closure of the defects (Table 4). Understanding the nature of interaction between these morphometric parameters and the device will be a crucial issue in efforts to reduce the incidence of residual defects following attempted closure.

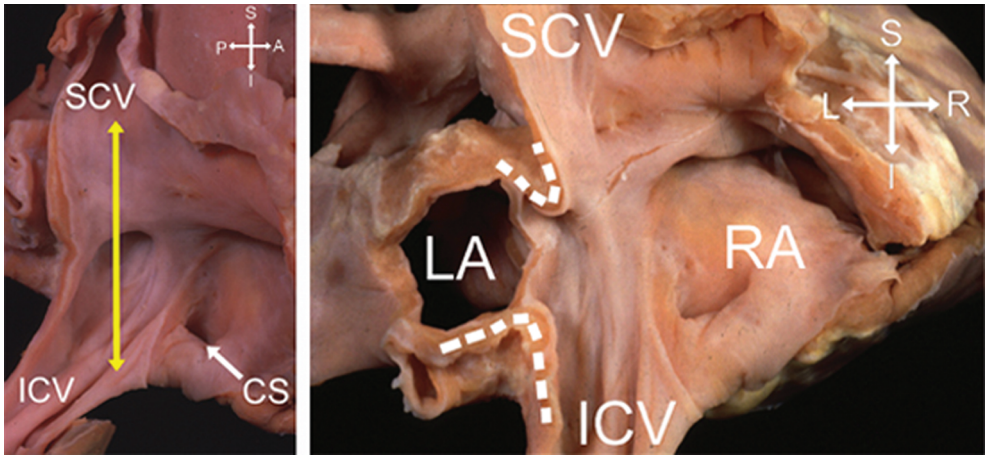

Figure 2.
The left panel shows the opened right atrium of a heart with an intact atrial septum. The yellow arrow indicates the 90-degree plane of section. In the right panel, the heart has been sectioned along the 90-degree plane. Dashed lines outline the infolded atrial free walls. The muscular portion of the true interatrial septum lies between the superior and inferior dashed lines. A: anterior; CS: coronary sinus; I: inferior; ICV: inferior caval vein; L: left; P: posterior; R: right; S: superior; SCV: superior caval vein.

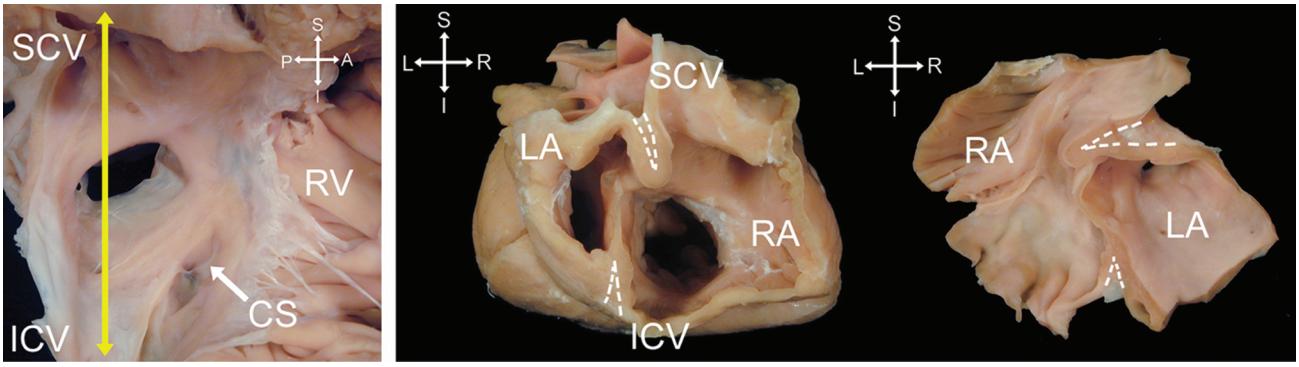

Figure 3.
The left panel shows the opened right atrium of a heart with a moderate sized atrial septal defect. The yellow arrow indicates the 90-degree plane of section. The superior rim of the defect is formed mainly of the infolded atrial free wall between the superior caval vein and left atrium (dashed lines, middle and right panels). Likewise, the inferior rim of the defect is formed of infolded atrial free wall between the inferior caval vein and left atrium. The right panel shows the posterior aspect of the heart, replicating the plane obtained by echocardiography. RV: right ventricle.

Comparison with previous studies

To our knowledge, this is the first study that has analyzed the efficiency of the Amplatzer device in relation to the morphology of the oval fossa. A recent study using the CardioSEAL device (4) attempted to determine echocardiographic predictors of successful closure in a group of 27 patients. Among other variables, deficiency of the superior rim proved a significant predictor of residual deficiencies at the level of univariate ($p = 0.03$), but not multivariate analysis. The CardioSEAL device, nonetheless, has a markedly different design when compared to the Amplatzer occluder.

In an earlier preliminary study using the Amplatzer device, we had found an association between multiple defects and the occurrence of residual defects. In this study, while we did find such an association at the exploratory, univariate stage ($p = 0.06$), no such association was found with multivariate analysis. It is conceivable, nonetheless, that the presence of one device may interfere with satisfactory effacement of the discs of a second device.

Limitations of the study

Both of our definitions of "failure" may be considered too strict, given the propensity of residual defects that are seen early after placement of a device to undergo spontaneous closure. The length of the superior rim, nonetheless, remained a significant predictor of failure in both models. We encountered a residual defect of hemodynamic significance in only

https://doi.org/10.1017/S1047951103000714 Published online by Cambridge University Press

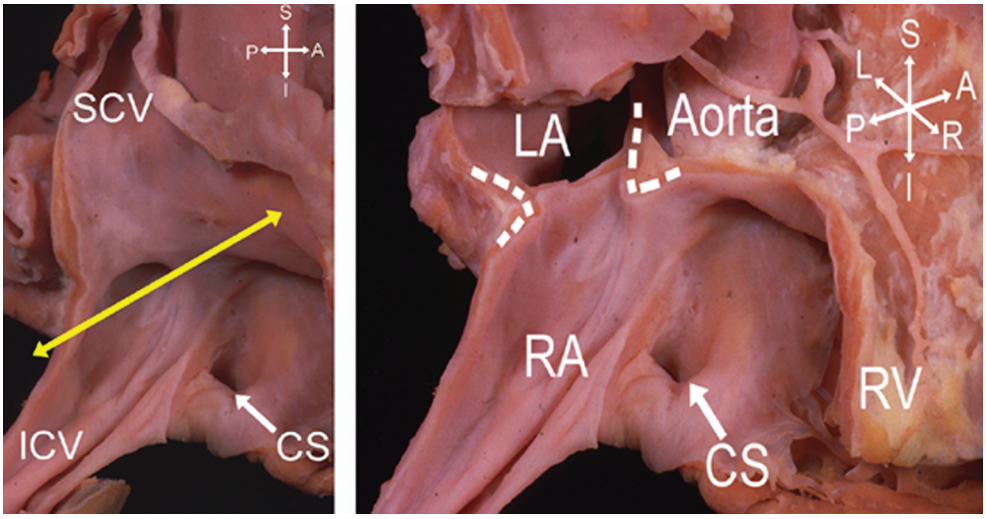

Figure 4.
The left panel shows the opened right atrium of a heart with an intact atrial septum. The yellow arrow indicates the 30-degree plane of section. In the right panel, this heart has been sectioned along the 30-degree plane. Dashed lines outline the infolded atrial free walls. The muscular portion of the true interatrial septum lies between the anterior and posterior dashed lines.

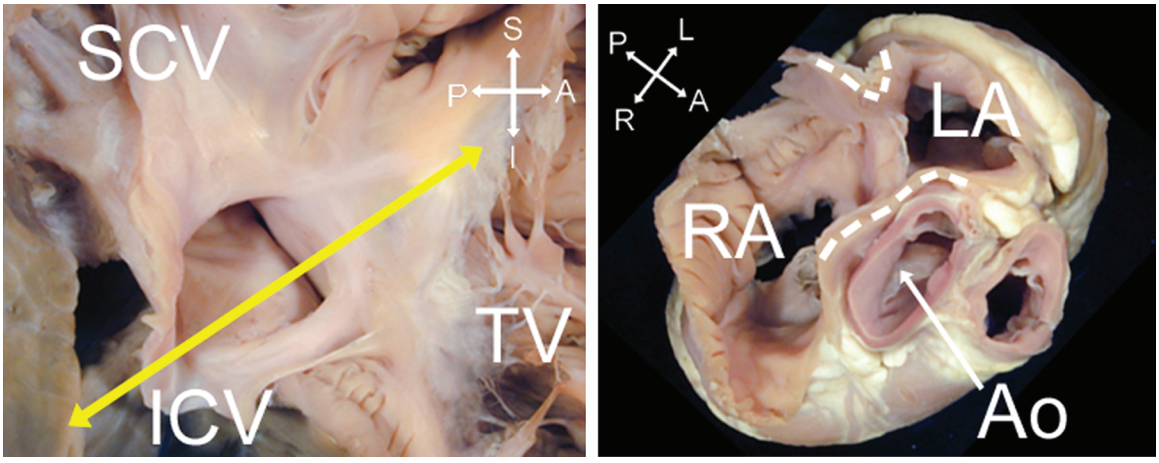

Figure 5.
The left panel shows the opened right atrium of a heart with a large atrial septal defect in the oval fossa. The yellow arrow indicates the 30-degree plane of section. The dashed lines outline the infolded atrial free walls. The muscular portion of the true interatrial septum lies between the anterior and posterior dashed lines. In this specimen, the anterior rim is severely attenuated. AO: aorta.

one patient. Pre-selection is inherent given the retrospective nature of the study. Selection bias may also be inherent within the constraints of a single-center study. Analysis of results from other centers may help to obtain a global perspective. Contrast echocardiography was not used to detect residual defects during follow-up.[4] This may explain why some residual defects were first detected at late studies. The number of patients with missing values for the width of the oval fossa at the 30-degree plane weakens the case for the true significance of this variable. We did not determine the mechanism for the occurrence of residual defects. In the future, real-time three-dimensional imaging during and after placement of the device may help clarify the interaction between the device, the mechanism of self-centering, and the topography of the atrial septum and adjacent structures. Finally, this study is applicable only to the Amplatzer device. Since individual devices differ in design, as well as mechanism of occlusion, separate studies are probably warranted for each device focusing on factors that may predispose to residual defects.

Conclusion

We have shown that it is possible to quantify morphometric echocardiographic parameters so as to predict occurrence of residual defects after closure of

https://doi.org/10.1017/S1047951103000714 Published online by Cambridge University Press

holes within the oval fossa using the Amplatzer device. Further understanding of the mechanisms by which these structures predispose patients to residual defects is needed. Such understanding will help improve selection of patients, design of the device, and ultimately to improved outcome from transcatheter closure of atrial septal defects.

References

1. Walsh KP, Maadi IM. The Amplatzer septal occluder. Cardiol Young 2000; 10: 493–501.
2. Carminati M, Giusti S, Hausdorf G, et al. A European multicentric experience using the CardioSEAL and Starflex double umbrella devices to close interatrial communications holes within the oval fossa. Cardiol Young 2000; 10: 519–526.
3. Godart F, Rey C, Francart C, et al. Experience in one center using the buttoned device for occlusion of atrial septal defect: comparison with the Amplatzer septal occluder. Cardiol Young 2000; 10: 527–533.
4. Momenah TS, McElhinney DB, Brook MM, Moore P, Silverman NH. Transesophageal echocardiographic predictors of successful transcatheter closure of defects within the oval fossa using the CardioSEAL septal occlusion device. Cardiol Young 2000; 10: 510–518.
5. Stumper O, Witsenburg M, Sutherland GR, Cromme-Dijkhuis A, Godman MJ, Hess J. Transesophageal echocardiographic monitoring of interventional cardiac catheterization in children. J Am Coll Cardiol 1991; 18: 1506–1514.
6. Tardif JC, Vannan MA, Pandian NG. Biplane and multiplane transesophageal echocardiography: methodology and echo-anatomic correlations. Am J Card Imaging 1995; 9: 87–99.
7. Seward JB. Biplane and multiplane transesophageal echocardiography: evaluation of congenital heart disease. Am J Card Imaging 1995; 9: 129–136.
8. Thanopoulos BD, Laskari CV, Tsaousis GS, Zarayelyan A, Vekiou A, Papadopoulos GS. Closure of atrial septal defects with the Amplatzer occlusion device: preliminary results. J Am Coll Cardiol 1998; 31: 1110–1116.
9. Sharafuddin MJA, Gu X, Titus JL, Umess M, Cervera-Ceballos JJ. Transvenous closure of secundum atrial septal defects. Preliminary results of a new self-expanding Nitinol prosthesis in a swine model. Circulation 1997; 95: 2162–2168.
10. Gutgesell HP, Rembold CM. Growth of the human heart relative to body surface area. Am J Cardiol 1990; 65: 662–668.
11. Martins JDF, Anderson RH. The anatomy of interatrial communications – what does the interventionist need to know? Cardiol Young 2000; 10: 464–473.